

Improving the d_{33} and g_{33} properties of 0-3 piezoelectric composites by dielectrophoresis

D. A. van den Ende,^{1,2,a)} B. F. Bory,¹ W. A. Groen,^{1,2} and S. van der Zwaag²

¹Department of Materials Technology, TNO Science and Industry, Rondon 1, 5612AP Eindhoven, The Netherlands

²Novel Aerospace Materials Group, Faculty of Aerospace Engineering, Delft University of Technology, Kluyverweg 1, 2629 HS Delft, The Netherlands

(Received 25 October 2009; accepted 12 December 2009; published online 25 January 2010)

Composites of piezoelectric particles in a polymer matrix with enhanced properties in the poling direction were prepared by dielectrophoretic alignment of the particles. The effect of processing parameters such as the amplitude and frequency of the applied electric field and the viscosity of the matrix on the dielectric and piezoelectric properties of the cured composite were demonstrated for a composite with a PZT volume fraction of 0.2. The amount of structuring could be correlated to the dielectric and piezoelectric properties of the composite through the P_2 order parameter for the average particle chain orientation, which was derived from image analysis of the microstructure. The piezoelectric properties of the aligned composites can be described with a new model for composites containing particles arranged into chains. The model predictions are in good agreement with the experimental results. © 2010 American Institute of Physics. [doi:10.1063/1.3291131]

I. INTRODUCTION

Piezoelectric materials are well suited as sensors in many applications, such as vibration monitoring, impact detection, and ultrasonic receiving sensors.¹⁻³ Piezoelectric composites consisting of a particulate piezoelectric ceramic phase randomly dispersed within a polymer matrix, generally referred to as 0-3 composites,⁴ are possible candidates for integrated sensors in structural composites.^{5,6} While displaying adequate mechanical properties, such composites exhibit intrinsically weak piezoelectric properties, such as a low piezoelectric charge coefficient (d_{33}) and only a moderate piezoelectric voltage coefficient (g_{33}).⁷⁻¹¹ These weak piezoelectric properties are the result of limited connectivity of the ceramic phase, which, in combination with a large discrepancy in dielectric properties for both phases, leads to an unfavorable electric field distribution in the composite.¹⁰

A beneficial higher connectivity can be achieved simply by utilizing very high volume fractions of piezoelectric ceramic powder in a 0-3 composite. However, this greatly reduces the mechanical failure strain while the increase in piezoelectric properties is limited. An alternative is the 1-3 type composite, in which continuous aligned fibers or precisely shaped pillars of piezoelectric material inside the matrix are employed.^{12,13} However, such systems typically involve intricate processing methods, often involving dicing a sintered block of ceramic or complex shaping of the delicate green ceramic mixture.¹⁴ The dielectrophoretic effect can be utilized to manipulate particles dispersed in a fluid medium¹⁵⁻¹⁸ and offers a simple alternative approach to create oriented particle filled polymer composites with anisotropic properties.¹⁹⁻²⁴ When an electric field is applied to an uncured thermosetting polymer, the dispersed particles form

chains, which are fixed in place when the matrix is cured. Several studies reporting an increase in the permittivity of a composite material in the direction of these chains have been published,²⁵⁻²⁹ However, the effect of the dielectrophoretic alignment on the piezoelectric properties, such as d_{33} and g_{33} , of piezoelectric particle-polymer matrix composites has not been explored yet, with the exception of one preliminary study.³⁰ In this paper, the effect of several key processing parameters on these piezoelectric properties and a quantitative coupling of these properties to the structured composites are investigated. Piezoelectric properties of structured composites with lead zirconate titanate (PZT) content volume fractions from 0.01 to 0.6 are investigated and compared to composites of randomly dispersed PZT particles. Experimental results are compared to the predictions of a new model for d_{33} as a function of PZT volume fraction of the composites and the correlation is discussed.

II. THEORY

A. Dielectrophoretic processing

Dielectrophoretically aligned composites can be obtained by applying an electric field to a composite medium of particles dispersed in an uncured thermosetting resin. The force acting on particles in a nonuniform electric field is known as the dielectrophoresis (DEP) force and can be utilized forming particle chains. The time averaged DEP force acting upon a dielectric sphere with a complex permittivity ϵ_2^* and radius r , suspended in a medium with a complex permittivity ϵ_1^* and subjected to an electric field E_{rms} , is equal to the root mean square value of the applied electric field:³¹

$$\langle F_{\text{DEP}} \rangle = 2\pi\epsilon_1' r^3 \text{Re}[K^*(\omega)] \nabla E_{\text{rms}}^2, \quad (1)$$

where ϵ_1' is the real part of the complex permittivity of the matrix and E_0 is the applied electric field. The complex Clausius–Mossotti function $K^*(\omega)$ is a function of the com-

^{a)}Author to whom correspondence should be addressed. Electronic mail: daan.vandenende@tno.nl.

plex permittivities ε_1^* , ε_2^* and of the direct current conductivities of both phases σ_1 , σ_2 of the ceramic particles and the polymer matrix, respectively, and of the angular frequency of the electric field ω , where $\omega = 2\pi f$.

$$K^*(\omega) = \frac{\varepsilon_2^* - \varepsilon_1^* - j(\sigma_2 - \sigma_1)/\omega}{\varepsilon_2^* + 2\varepsilon_1^* - j(\sigma_2 + 2\sigma_1)/\omega}. \quad (2)$$

This function must be positive in order to obtain dielectrophoretically formed chains of significant length and aligned parallel to the direction of the electric field. The sign and magnitude of this function are dependent on the frequency of the applied electric field.

Other forces controlling the motion of the particles in a fluid are thermal noise and gravitational forces.²⁵ However, these effects were not taken into account for this research as the epoxy is cured at low temperature and no sedimentation was observed.

Another important parameter affecting the alignment of the particles is the viscosity of the polymer matrix. An increase in viscosity results in a higher drag force acting on the particles. The drag force can be approximated using Stokes' law for flow at low Reynolds numbers,

$$F_{\text{drag}} = 6\pi\eta vr, \quad (3)$$

where η is the viscosity of the medium, r is the radius of the particle, and v is the velocity of the particle. The velocity at which the particles travel is determined by the equilibrium between time averaged DEP and drag forces, when $\langle F_{\text{DEP}} \rangle - F_{\text{drag}} = 0$, as generally the time dependent forces are damped by the fluid viscosity for micron sized particles.³¹ Thus, an increase in viscosity leads to a lower particle velocity, delaying alignment. In a thermosetting matrix, limited time will be available before the matrix solidifies at which point particles are definitively immobilized. Therefore, the speed at which particles align is an important factor influencing the final piezoelectric properties of the composites.

B. Modeling of piezoelectric properties

The unstructured 0-3 composite system of randomly dispersed particles in a polymer matrix is considered as reference system. The model described in Eq. (4) is Yamada's model for ellipsoidal particles in an isotropic matrix.⁷ The dielectric constant of the composite is given by

$$\varepsilon = \varepsilon_1 \left(1 + \frac{n\varphi(\varepsilon_2 - \varepsilon_1)}{n\varepsilon_1 + (\varepsilon_2 - \varepsilon_1)(1 - \varphi)} \right), \quad (4)$$

where ε is the permittivity of the composite, ε_1 and ε_2 are the permittivities of the matrix and the particles, respectively, φ is the volume fraction of ceramic powder in the composite, and n is the inverse of the depolarization factor for an ellipsoidal particle in the direction of the applied electric field. This model is an alternative representation of the unified mixing rule for ellipsoidal particles.³² In all equations concerning modeling of the cured composites, the materials are considered to be loss free, both in electrical and mechanical sense.

The effective d_{33} constant of the 0-3 composite is then

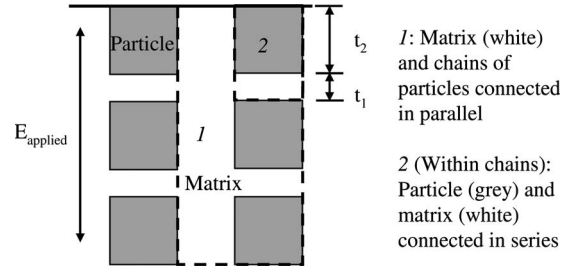


FIG. 1. Model schematic for the effective permittivity of a structured piezoelectric composite representing aligned particles (gray) in a matrix (white) (after Ref. 27).

$$d_{33} = \varphi \frac{n\varepsilon}{n\varepsilon(\varepsilon_2 - \varepsilon)} d_{33_2}, \quad (5)$$

where d_{33_2} is the piezoelectric voltage constant of the ceramic particles. Structured particles will experience different interactions than randomly dispersed particles. Within the chains, aligned particles will experience strong interactions in the direction of the alignment, whereas in the regions without particles, there is only the matrix to consider. This alters the structure of the composites to one resembling the 1-3 alignment. An analytical model for the permittivity of structured samples is presented by Bowen *et al.*²⁷ The model considers cubic particles within perfectly aligned chains as capacitors in series, which are in turn connected in parallel to the matrix region outside of the chains, which is depleted of particles. A schematic diagram of the configuration is shown in Fig. 1.

The equations for the permittivity for such a composite are as follows:²⁷

$$\varepsilon_{\text{DEP}} = \varphi \left[\frac{R\varepsilon_1\varepsilon_2}{\varepsilon_2 + R\varepsilon_1} \right] + (1 - \varphi)\varepsilon_1, \quad (6)$$

where ε_{DEP} is the permittivity of the dielectrophoretically aligned composite and $R = t_2/t_1$ is the ratio of the average particle size divided by the effective interparticle distance.

This model can be expanded to include electromechanical coupling to obtain the composite d_{33} by modeling the particle-matrix alternations in the chains as two capacitors in series in the electrical domain and two springs in series in the mechanical domain. This electromechanical representation of the chains is substituted for the active piezoelectric part of a 1-3 composite model.³³ The equations for d_{33} of this 1-3 composite model are given in

$$d_{33} = \frac{\varphi S_1}{\varphi S_1 + (1 - \varphi)S_{33_2}} d_{33_2}, \quad (7)$$

where S_1 and S_{33_2} are the compliances of the (isotropic) polymer and ceramic in the poling direction, respectively, and d_{33_2} is the piezoelectric charge constant of the ceramic in the poling direction.

The electric field acting on the particle E_2 , relative to the applied electric field E_{app} , can be described using the size ratio R , as defined in Eq. (6), and the permittivity of both phases, by treating the particle and matrix as two capacitors connected in series:

$$\frac{E_2}{E_{app}} = \frac{(1+R)\varepsilon_1}{\varepsilon_2 + R\varepsilon_1}. \quad (8)$$

From Eq. (8), the effective d_{33} of the chains of particles (d'_{33_2}), as a result of this series connectivity of the particles inside these chains, can be determined:

$$d'_{33_2} = \frac{E_2}{E_{app}} \quad d_{33_2} = \frac{(1+R)\varepsilon_1}{\varepsilon_2 + R\varepsilon_1} d_{33_2}. \quad (9)$$

In addition to the electrical coupling determined in Eq. (9), the equivalent compliance of the chains, S'_{33_2} , is presented in Eq. (10)

$$S'_{33_2} = \frac{Y_{33_2} + RY_1}{(1+R)Y_1Y_{33_2}}, \quad (10)$$

where Y_1 and Y_{33_2} are the elastic moduli of the polymer matrix and of the ceramic in the direction of the chains. Combining Eqs. (7), (9), and (10) yields an equation for $d_{33_{DEP}}$, the d_{33} of the dielectrophoretically structured composite:

$$\begin{aligned} d_{33_{DEP}} &= \frac{\varphi S_1}{\varphi S_1 + (1-\varphi)S'_{33_2}} d'_{33_2} \\ &= \frac{(1+R)^2 \varepsilon_1 \varphi Y_{33_2} d_{33_2}}{(\varepsilon_2 + R\varepsilon_1)[(1+R\varphi)Y_{33_2} + (1-\varphi)RY_1]}. \end{aligned} \quad (11)$$

III. EXPERIMENTAL

A. Materials

A two component epoxy system (Epotek 302-3M, Epoxy Technology Inc., Billerica, MA), based on diglycidyl ether of bisphenol-A (DGEBA) resin and poly(oxypropyl)-diamine (POPD) multifunctional aliphatic amine curing agent, was used. The PZT powder used in this study was a powder which is used industrially for PZT5A4 ceramics (Morgan Electroceramics, Ruabon, UK). The as received powder was further calcined at 1150 °C for 1 h to improve its piezoelectric properties. The agglomerated powder was milled to a micrometer range size distribution (around 1–10 μm) by using a motorized pestle and mortar (Retsch MS). The powder was stored in an air ventilated drying oven at 150 °C to avoid adsorption of moisture. The particle size distribution of the calcined and milled powder was measured using a Beckman Coulter LS230 laser diffraction particle size analyzer. Particles were dispersed into an aqueous solution stabilized by sodium phosphate. The particle size distribution was found to be $d_{10}=0.94 \mu\text{m}$, $d_{50}=3.4 \mu\text{m}$, and $d_{90}=7.9 \mu\text{m}$.

The epoxy resin and ceramic particles were mixed together using a planetary mixer (SpeedMixer DAC 150 FVZ, Hauschild). The PZT particles were dispersed in the resin component of the epoxy, by mixing at 3000 rpm for 3 min. Subsequently, the hardener was added and the composite resin was again mixed at 3000 rpm for 5 min, followed by degassing in vacuum for 10 min. The composite resin was then poured into a mould (see Fig. 2), consisting of a Teflon spacer of 500 μm thickness and a 16 mm diameter cut-out, with two layers of 50 μm thick aluminum foil placed on

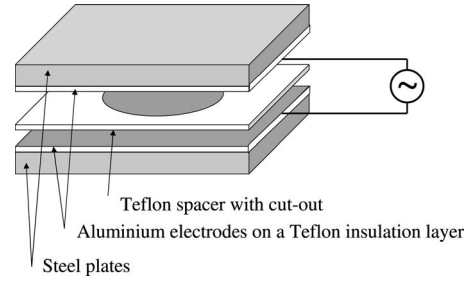


FIG. 2. Schematic drawing of the mould used for curing the composite under an applied electric field.

both sides of the spacer, acting as electrodes for the structuring field. The system is bolted between two steel plates to apply pressure to the mould. Additional Teflon layers separate the electrodes from the steel backing plates.

A signal generator (Tektronix AFG320) was coupled to a high voltage amplifier (Radiant Tech, RT6000 HVA-2) for applying the electric field. The electric field was applied immediately after the mould was placed on a hotplate while heating to a fixed temperature of 55 °C. The electric field was applied for a minimum of 3 h at this temperature before cooling the mould to room temperature and removing the electric field. Samples of 0.5 mm thickness with a PZT volume fraction of 0.2 were processed under sinusoidal electric fields with amplitudes up to $E_{pk}=1500 \text{ V}_{pk}/\text{mm}$ and frequencies of up to $f=100 \text{ kHz}$ to investigate the effects of processing on structuring. The input voltage was corrected for any attenuation caused by the amplifier at higher frequencies. Samples with a variable PZT fraction up to 0.6 were processed at a fixed electric field of $E_{pk}=500 \text{ V}_{pk}/\text{mm}$ and $f=4 \text{ kHz}$ to determine compositional effects.

The effect of matrix viscosity on the degree of alignment during dielectrophoretic structuring was determined by pre-curing the composite for various times at room temperature. Subsequently the mould was transferred to the hotplate and structuring electric field was applied to allow dielectrophoretic alignment to commence. The minimum viscosity of the epoxy during the structuring was determined by simulating the heating profile in a rheometer (Anton Paar, Physica MCR301) and simultaneously measuring the viscosity of the resin. The randomly dispersed samples were cured using a similar mould without applying the electric field. During curing of these samples, the mould was rotated at a speed of about 2–3 rotations/min. The rotating mould was placed in an oven and heated to a temperature of 55 °C. All samples were postcured 1 h at 100 °C before sputtering 12.5 mm diameter circular gold electrodes on both sides (Edwards 150SB Sputtercoater). Poling was performed at 10 kV/mm at 100 °C in a silicone oil bath for a duration of 30 min. The poling field was only removed after cooling to room temperature. Dielectric measurements were performed at 1 kHz using an LCR meter (HP 4284A). Finally, d_{33} measurements were performed with a Berlincourt type d_{33} meter (PM3000, PiezoTest, UK).

The microstructure of the sample was observed using a scanning electron microscopy (SEM) (FEI Quanta 600) operated in secondary electron imaging mode. Samples sectioned parallel to the chains were embedded into a room

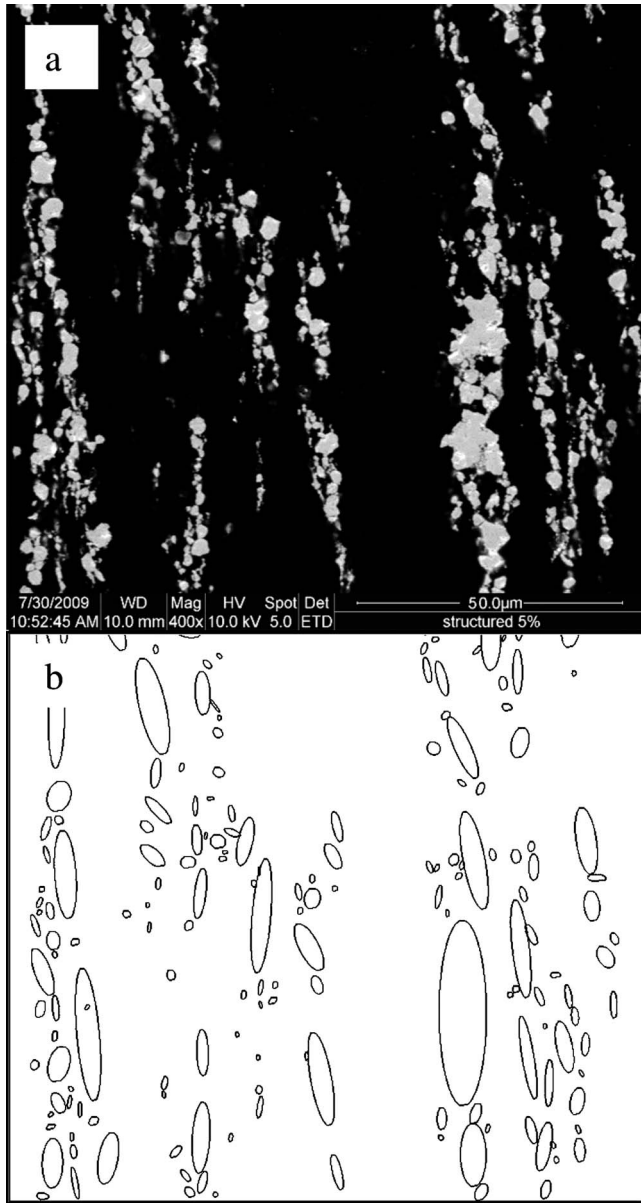


FIG. 3. SEM micrograph of a structured PZT/epoxy composite with a PZT volume fraction of 0.05 (a) and equivalent fitted ellipses (b).

temperature curing epoxy and polished with a 1 μm diamond paste. The SEM images of sample cross sections were analyzed using the software IMAGEJ.³⁴ First, the image was processed to enhance the contrast between the matrix (black) and the PZT particles (white). Then, ellipses were fitted to regions of PZT particles in direct contact. Details of the fitting procedure are described elsewhere.³⁵ Finally, the angle, β , between the major axis of the ellipsoid and the direction of the applied electric field was determined. A typical SEM micrograph of a partially aligned sample and the equivalent image of fitted ellipses are presented in Fig. 3.

The degree of geometric alignment of the particles can be quantified by calculating an order parameter. A common order parameter is the \overline{P}_2 order parameter, which is used to quantify the average orientation of rodlike molecules, for instance, in liquid crystal phase analysis.³⁶

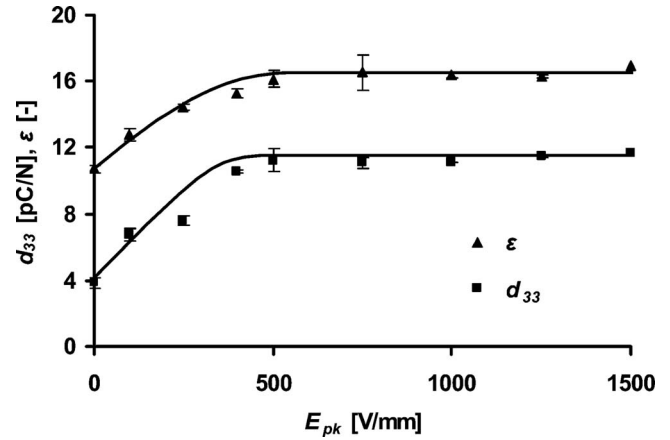


FIG. 4. The d_{33} and ϵ values obtained for structuring electric field amplitudes up to 1500 V_{pk}/mm at a fixed frequency of 4 kHz.

$$\overline{P}_2 = \frac{3}{2} \cos^2 \beta - \frac{1}{2}. \quad (12)$$

The \overline{P}_2 order parameter takes the value $\overline{P}_2=0$ for an isotropic phase, i.e., for a random sample. In the case of a fully aligned microstructure, the average value is $\overline{P}_2=1$.

IV. RESULTS

A. Processing parameters

The ϵ and d_{33} dependences on the amplitude of the structuring electric field, for a composite with 0.2 volume fraction PZT, are shown in the Fig. 4. Both properties increase with the applied electric field in the range measured up to a maximum value of $\epsilon=16$ and $d_{33}=11$ pC/N, respectively, which is achieved at around 500 V_{pk}/mm . No breakdown was observed for this range of electric field amplitudes at any time during the processing.

The effect of the frequency of the electric field, at a fixed applied field of 500 V_{pk}/mm , on the d_{33} and ϵ , is presented in Fig. 5. The highest values are found at a frequency of 4 kHz. At low frequencies, the d_{33} and ϵ values drop to those measured for composites with randomly dispersed particles. At frequencies above 4 kHz, the values also decrease.

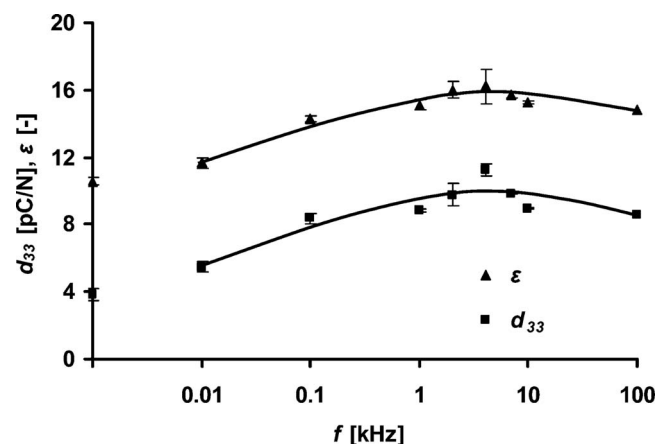


FIG. 5. The d_{33} and ϵ obtained for different frequencies at an applied field of 500 V_{pk}/mm . The d_{33} and ϵ values measured for 0-3 composites are marked on the y-axis.

TABLE I. The viscosity of the Epotek 302-3M epoxy at the end of the precuring stage, η_{start} , and the minimum viscosity reached during the curing cycle, η_{min} .

Precuring time (min)	η_{start} (Pa s)	η_{min} (Pa s)
0	2.11	0.75
28	4.01	1.3
60	11.3	2.9
100	29.6	5.2
144	102	13.1
224	1050	65.5
305	10 200	508

The viscosity of the matrix epoxy after various precuring times is presented in Table I. The viscosity values at the end of the precuring stage, η_{start} , as well as the minimum viscosity value during the curing cycle, η_{min} , are given. The ϵ and d_{33} values of the resulting composites decrease logarithmically with η_{min} . This relation is presented in Fig. 6, in which the ϵ and d_{33} values of 0-3 composites are depicted by the dotted lines.

B. Volume fraction of PZT

In Fig. 7, the permittivity results are presented for PZT volume fractions from 0.01 to 0.6. The composites were processed at a fixed applied field of $E_{\text{pk}}=500 \text{ V}_{\text{pk}}/\text{mm}$ and $f=4 \text{ kHz}$. The ϵ values that were measured for the dielectrophoretically structured samples are higher than those for 0-3 composites for the complete range of PZT volume fractions.

The influence of dielectrophoretic structuring on d_{33} constants of the composites is presented in Fig. 8. A clear difference can be observed between random and structured samples, especially at low PZT volume ratio.

V. DISCUSSION

The ϵ and d_{33} results obtained show that by aligning the particles, an increase in dielectric and piezoelectric properties can be obtained while keeping the volume fraction of PZT constant. The amount of increase depends on amplitude and frequency of the applied field and on the viscosity of the

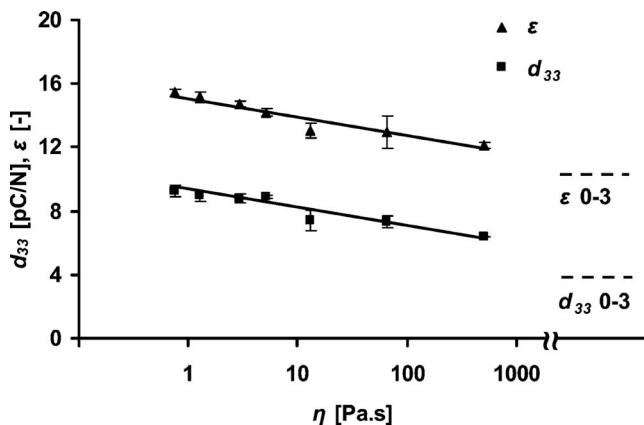


FIG. 6. The d_{33} and ϵ values obtained for different minimum viscosities of the epoxy after applying an electric field of $500 \text{ V}_{\text{pk}}/\text{mm}$ at 4 kHz . The d_{33} and ϵ values measured for 0-3 composites are marked by the dotted lines.

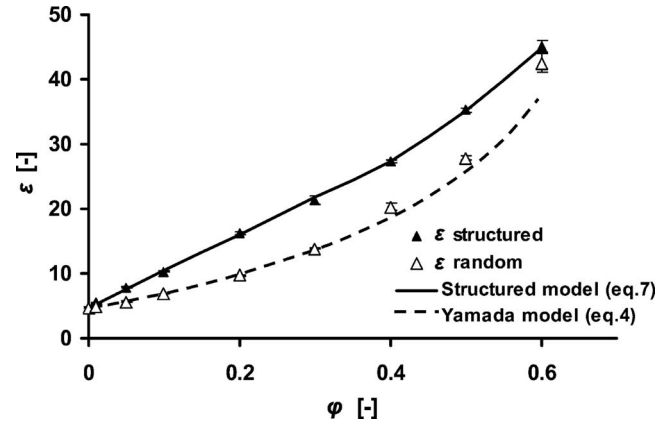


FIG. 7. Measured permittivity values for both structured and random configuration with their associated analytical model from 0 to 0.6 volume fraction of PZT. The solid lines indicate the fitted model predictions.

polymer matrix. When the amplitude of the applied field is increased, an initial increase in properties is witnessed. This is due to the increase in the DEP force with applied field [see Eq. (1)], leading to more alignment. Saturation is achieved when all particles are in contact and are trapped in a (local) minimum energy states before the matrix is completely cured. At $\phi=0.2$, this occurs at around $E_{\text{pk}}=500 \text{ V}_{\text{pk}}/\text{mm}$ for $f=4 \text{ kHz}$. Wilson *et al.*²⁵ studied the effect of processing parameters on dielectrophoretic alignment of PbTiO_3 in Epotek 302-3M epoxy by visual observations at low ceramic volume fractions. Results from that study indicate poor alignment at electric fields above $500 \text{ V}_{\text{pk}}/\text{mm}$ and frequencies up to 4 kHz . This was primarily attributed to electrohydrodynamic flow of the epoxy. However, these observations were snapshots and limited to the early stages of the cure, whereas the results presented in Fig. 4 represent final values of ϵ and d_{33} . It is thus possible that electrohydrodynamic flow occurs during early stages of the cure when the epoxy system has the highest dielectric loss.³⁷ At a later stage in the cure, the dielectric loss decreases, allowing the dielectrophoretic alignment of particles and the corresponding increase in properties to commence.

The effect of frequency can be explained as follows: At low frequencies the conductivity of the epoxy prohibits ef-

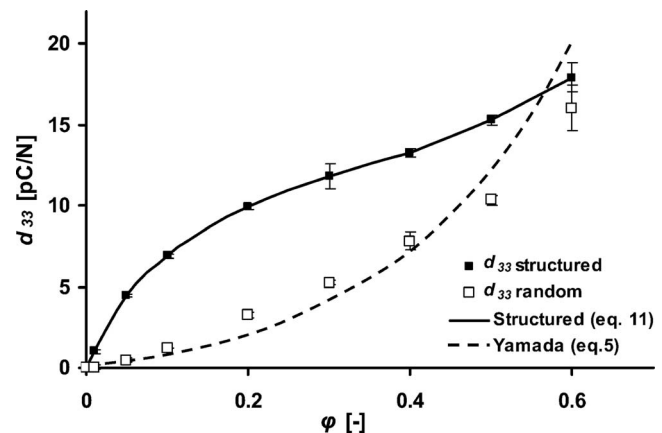


FIG. 8. Measured d_{33} values for both structured and random composites with their associated analytical model from 0 to 0.6 volume fraction of PZT. The solid lines indicate the fitted model predictions.

TABLE II. Comparison for the estimated the time to contact for two particles, starting at an initial separation distance of 2 μm .

Precurring time (min)	η_{\min} (Pa s)	ε_1 ($f=4$ kHz)	$\langle F_{\text{DEP}} \rangle^a$ (N)	v^a (m/s)	Average time to contact (s)
0	0.75	6.7	1.36×10^{-11}	5.7×10^{-7}	1.2
100	5.2	4.8	9.83×10^{-12}	5.9×10^{-8}	10.6
305	508	4.5	9.23×10^{-12}	5.7×10^{-10}	1086

^aBoth the DEP force and the particle velocity increase with a decreasing separation distance, only the initial values are given in this table.

fective structuring, as $K \ll 1$ at low frequencies [see Eq. (2)]. This results in less than optimal ε and d_{33} values. But even at a frequency of 10 Hz, d_{33} values are significantly higher than the values for randomly dispersed particle composites. Both Bowen *et al.*²⁴ and Wilson *et al.*²⁵ observed no dielectrophoretic alignment of piezoelectric ceramic particles below 1 kHz in epoxy systems at low ceramic volume fractions. Again, these visual measurements were performed in early stages of the cure. Evidently the structuring commences at a later stage in the cure, primarily because K increases as a result of decreasing conductivity of the resin.³⁷ At frequencies above 10 kHz, the conductivity of the epoxy is negligible (i.e., $K \rightarrow 1$) and the DEP force is governed by the frequency dependence of the permittivity of the matrix, ε'_1 [see Eq. (1)]. At these frequencies, molecular relaxations cannot follow the direction of the electric field. As a result, ε'_1 decreases^{25,38} and, correspondingly, the DEP force.

The viscosity of the epoxy and the amount of structuring are inversely related. Based on Eq. (3), an increase in viscosity leads to an increase in the drag force and thus to a decrease in particle velocity. Therefore, the time needed for alignment of the particles increases. If the particles are not fully aligned when the polymer solidifies, the resulting piezoelectric properties of the composite will be inferior. When a structuring field is applied to a fully cross-linked matrix (i.e., $\eta \rightarrow \infty$), the ε and d_{33} values of a 0-3 composite will result (dotted lines in Fig. 6). An estimate for the average time to contact for two particles can be approximated from the equilibrium particle velocity, starting from the average separation distance of the average sized particles, approximated at 2 μm for a 0.2 volume fraction of PZT. This velocity is found from Eqs. (1) and (3) by calculating $\langle F_{\text{DEP}} \rangle - F_{\text{drag}} = 0$. In Table II, the estimated time to contact for two particles is given for three different precurring times, assuming the viscosity of the epoxy is constant at the minimum value for the given precurring time. The applied electric field was set at 500 $\text{V}_{\text{pk}}/\text{mm}$. The permittivity of the matrix is estimated from dielectric data measured for the Epotek 302-3M system during the curing cycle.²⁵ A point dipole approximation is used for estimation of the induced electric field due to the concentration of the applied electric field around the particles.³⁹

The actual contact time in actual composite systems may deviate from the estimates in Table II as the point dipole approximation is known to become incorrect when particles approach each other closely.⁴⁰ Furthermore, the particle size distribution and variations in initial separations can influence DEP interactions to a great extent causing local fluctuations

in time to contact between particles, especially when interactions between more than two particles are considered. As can be seen in Table II, the initial DEP force between particles for a precurring time of 300 min is around 70% of the initial DEP force for a precurring time of 0 min, while the initial particle velocity is reduced to 0.15% of the original value. The increase in time to contact of almost a factor 1000 is therefore primarily the result of the increase in viscosity of the matrix. The high viscosity matrix hampers particle chain formation in the composites. However, even at the longest precurring time of 305 min, the resulting d_{33} value of these composites is still higher than the d_{33} value of the 0-3 composites, indicating that alignment still occurs to some extent.

In Fig. 9, the values of the geometrical order parameter, \overline{P}_2 , for composites processed with varying voltage, frequency, and viscosity are plotted versus the ε and d_{33} values of the composites. The results presented in Fig. 9 reveal a clear and unique dependence: both ε and d_{33} are correlated to the \overline{P}_2 order parameter and increase with this factor. No difference was found in the relation between \overline{P}_2 and ε and d_{33} for the differently processed series, indicating independent correlation of \overline{P}_2 to the degree of alignment and therefore to the final dielectric and piezoelectric properties. The slope and y-axis intersect point of the line are expected to depend on the volume fraction of PZT in the composite and the morphology of the particles.

The \overline{P}_2 value is based on the geometrical orientation of the particles, the angle β , which is relatively insensitive to deviations brightness and contrast settings in the SEM images and threshold gray value settings during analysis. Con-

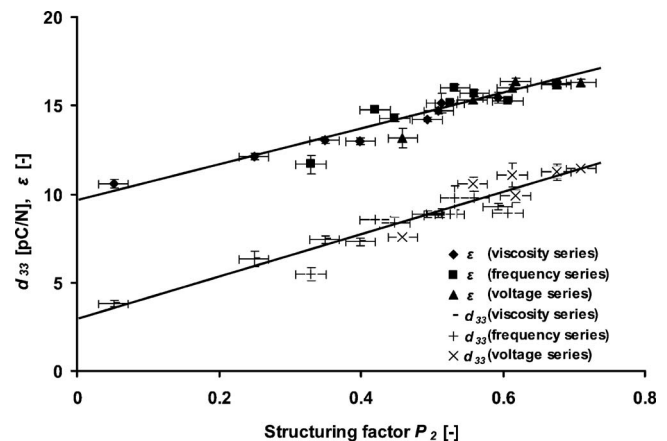


FIG. 9. The d_{33} and ε obtained for different viscosities, frequencies, and voltages, plotted against the order parameter calculated from SEM pictures. The lines have been added as a guide for the eye.

sidering an error of ± 25 in the chosen threshold grey values in the same image (i.e., $\pm 10\%$ on a scale of 0–255), an average difference in \overline{P}_2 value of only 0.021 was calculated (i.e., only $\sim 2\%$ for a completely structured sample). This conservative estimate of the error was found to be independent of the actual value of the \overline{P}_2 order parameter.

In Figs. 7 and 8, Yamada's model for ε and d_{33} for 0-3 composites, as described in Eqs. (4) and (7) and the model for dielectrophoretically processed composites, as described in Eqs. (6) and (11), are plotted. The permittivity values for each of the phases were measured on pure epoxy samples and bulk PZT ceramic samples and were measured to be $\varepsilon_1=4.76$ and $\varepsilon_2=1850$, respectively. The d_{33} of the ceramic phase was measured to be $d_{33,2}=420$ pC/N. It is assumed that the piezoelectric properties of the particles are equal to the bulk ceramic values, as particle properties could not be measured directly. The mechanical properties of the phases were taken from manufacturer datasheets, the stiffness of the epoxy $Y_1=1.7$ GPa, and the stiffness of the ceramic in the poling direction $Y_{33,2}=70$ GPa. The curves corresponding to Yamada's model were obtained using a value of $n=4.56$, which corresponds to randomly oriented ellipsoids with a:b:c=3:1:1.³² The values for both ε and d_{33} of the composites match reasonably well to the model, indicating that the composites with randomly dispersed particles are indeed true 0-3 composites. The effect of dielectrophoretic structuring on ε and d_{33} is found to be most pronounced at lower PZT volume fractions. The improvement effect of DEP is less marked at higher volume fractions and the difference in properties has all but vanished at a volume fraction of 0.6. At high volume fractions, the particles are more likely to be constrained in their movement as the majority of particles are already in contact before the electric field is applied and differences in the degree of contact alignment become small at high PZT volume fractions, well above the percolation threshold. The trend of a linear increase in ε and an initially rapidly increasing d_{33} is coherent with theory for anisotropic piezoelectric particles, such as chains or pillars, spanning the length of the composites in a 1-3 type fashion.³³ However, the slope of the increase in both properties is much lower than true 1-3 ceramic-polymer composites, owing to the fact that the properties of the chains are governed by the weakest phase, both in mechanical and electrical sense. In both aspects, this accounts to the polymer phase in the composite.

In Eqs. (6) and (11), the ratio, R , of interparticle distance over the particle size in the direction of the electric field is an important parameter influencing the fraction of the applied electric field acting on the ceramic particles. The interparticle distances have been estimated by fitting the model to the data and are presented in Fig. 10, both for the structured composites and the reference 0-3 composites.

The estimated interparticle distances from ε and d_{33} values decrease with the PZT volume fraction in the composites. Furthermore, the estimated interparticle distances from ε and d_{33} values yield similar results, indicating that the parallel chains model [Eq. (11)] provides a reasonable representation of structured composites. The estimated distances correlate well to the observed microstructure of the composites, indicating that the estimated ε_2 and $d_{33,2}$ are reasonable. With

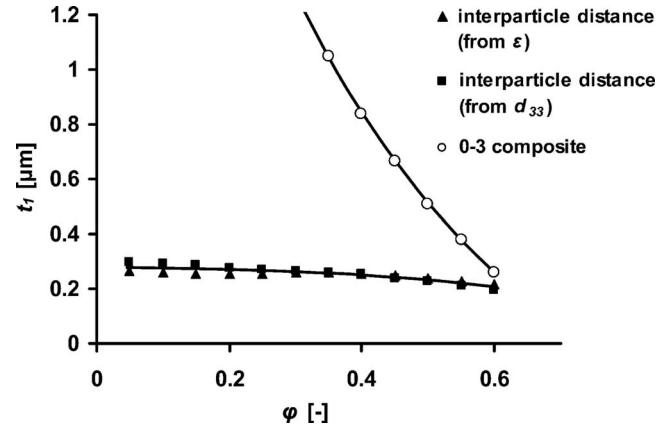


FIG. 10. Estimated values of the average interparticle distance, obtained by fitting model predictions to the measured ε and d_{33} values. The average interparticle distance for a randomly dispersed 0-3 composite is added for reference.

increasing φ , the increasing volume occupied by the particles causes them to become more closely packed in every direction, which is represented in the model by an increase in the ratio R . A comparison is made with the average interparticle distances in a 0-3 composite of randomly oriented, evenly spaced cubic particles. It can be seen that the parallel chain model predicts a lower interparticle distance for the dielectrophoretically structured composites up to a PZT volume fraction of 0.6.

The g_{33} values can be calculated and are shown in Fig. 11, by dividing the d_{33} of the composite by its permittivity, ε . The maximum value obtained for random samples is 43.5 mVm/N, at a PZT fraction of 0.4, while for structured composite, a value of 75 mVm/N is reached. In addition, this maximal value obtained by dielectrophoretic structuring is at a PZT volume fraction of 0.1. At higher volume fractions, the improvement in g_{33} properties decreases rapidly. The behavior of the g_{33} constant resembles the behavior witnessed in true 1-3 composites, where a maximum is also obtained at a low volume fraction⁴¹ (around 0.05 for a PZT5A4 fiber-polymer system³³). In both cases, the derivative of d_{33} decreases to zero with increasing φ , while the derivative of ε is constant, leading to a maximum in g_{33} at the volume fraction for which both derivatives are equal. The magnitude and posi-

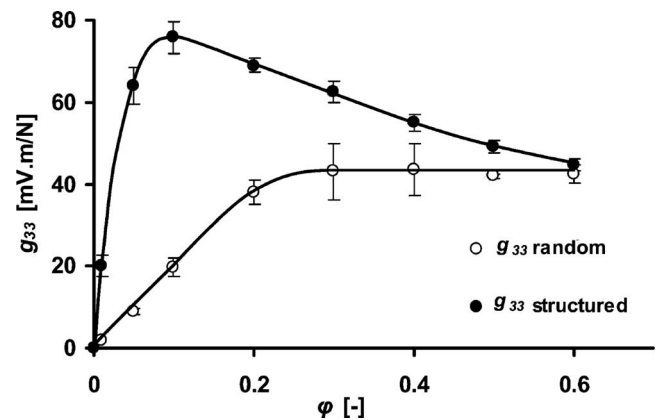


FIG. 11. The g_{33} values for structured and random sample from 0 to 0.6 volume fraction of PZT calculated from the measured d_{33} and ε values.

tion of the maximum depends on the stiffness ratio of the piezoelectric phase over the polymer matrix. For very stiff PZT, the initial increase in d_{33} is more rapid and a higher maximum g_{33} is obtained at a lower the volume fraction. For structured composites, a higher R corresponds to a higher stiffness. The benefits of having a maximum sensitivity at a low volume fraction are manifold and cover aspects such as price, density, and mechanical flexibility.

VI. CONCLUSIONS

This work shows that a significant increase in piezoelectric properties of 0-3 composites can be achieved by dielectrophoretic alignment of the piezoelectric particles inside a polymer matrix. The degree of alignment can be controlled by varying processing parameters and quantified by analyzing the composite cross section. The order parameter, P_2 , of the aligned particle chains correlates linearly with the increase in dielectric and piezoelectric properties of the composites, irrespective of the processing method used to influence the alignment. Whether this relationship holds for composites with higher PZT volume fractions must be further investigated. The dielectrophoretic alignment results in an increase in piezoelectric properties compared to 0-3 composites, especially at low volume fractions. As a result, sensitivity is increased and the maximum g_{33} occurs at a lower volume fraction of PZT, leading to other favorable properties such as a higher flexibility and a lower density of the composite.

ACKNOWLEDGEMENTS

This work was financially supported by the Smartmix funding program (Grant No. SMVA0607), as part of the program "Smart systems based on integrated Piezo." The authors are grateful to Morgan Electro Ceramics (Ruabon, United Kingdom) for providing the PZT powder and to Indu Babu and Professor Bert de With (SMG group, Eindhoven University of Technology), for the use of their Berlincourt d_{33} meter.

¹S. M. Peelamedu, C. Ciocanel, and N. G. Naganathan, *Smart Mater. Struct.* **13**, 990 (2004).

²M. Lin and F. K. Chang, *Compos. Sci. Technol.* **62**, 919 (2002).

³S. Bhalla and C. K. Soh, *J. Aerosp. Eng.* **17**, 154 (2004).

⁴R. E. Newnham, D. P. Skinner, and L. E. Cross, *Mater. Res. Bull.* **13**, 525 (1978).

⁵R. A. Badcock and E. A. Birt, *Smart Mater. Struct.* **9**, 291 (2000).

⁶M. P. Wenger, P. Blanas, R. J. Shuford, and D. K. Das-Gupta, *Polym. Eng.*

Sci. **36**, 2945 (1996).

⁷T. Yamada, T. Ueda, and T. Kitayama, *J. Appl. Phys.* **53**, 4328 (1982).

⁸G. Sa-Gong, A. Safari, S. J. Jang, and R. E. Newnham, *Ferroelectr., Lett. Sect.* **5**, 131 (1986).

⁹C. J. Dias and D. K. Das-Gupta, *IEEE Trans. Dielectr. Electr. Insul.* **3**, 706 (1996).

¹⁰A. Safari, *J. Phys.* **III 4**, 1129 (1994).

¹¹K. S. Lam, Y. Zhou, Y. W. Wong, and F. G. Shin, *J. Appl. Phys.* **97**, 104112 (2005).

¹²M. Schwartz, *Smart Materials* (CRC, Boca Raton, FL, 2008).

¹³R. Kar-Gupta, C. Marcheselli, and T. A. Venkatesh, *J. Appl. Phys.* **104**, 024105 (2008).

¹⁴A. Safari, M. Allahverdi, and E. K. Akdogan, *J. Mater. Sci.* **41**, 177 (2006).

¹⁵H. A. Pohl, *J. Appl. Phys.* **22**, 869 (1951).

¹⁶W. M. Winslow, *J. Appl. Phys.* **20**, 1137 (1949).

¹⁷T. Hao, *Adv. Colloid Interface Sci.* **97**, 1 (2002).

¹⁸L. An and C. R. Friedrich, *J. Appl. Phys.* **105**, 074314 (2009).

¹⁹C. A. Randall, D. V. Miller, J. H. Adair, and A. S. Bhalla, *J. Mater. Res.* **8**, 899 (1993).

²⁰C. A. Randall, S. Miyazaki, K. L. More, A. S. Bhalla, and R. E. Newnham, *Mater. Lett.* **15**, 26 (1992).

²¹C. P. Bowen, T. R. Shrout, R. E. Newnham, and C. A. Randall, *J. Intell. Mater. Syst. Struct.* **6**, 159 (1995).

²²C. P. Bowen, A. S. Bhalla, R. E. Newnham, and C. A. Randall, *J. Mater. Res.* **9**, 781 (1994).

²³C. Park and R. E. Robertson, *J. Mater. Sci.* **33**, 3541 (1998).

²⁴C. P. Bowen, T. R. Shrout, R. E. Newnham, and C. A. Randall, *J. Mater. Res.* **12**, 2345 (1997).

²⁵S. A. Wilson, G. M. Maistros, and R. W. Whatmore, *J. Phys. D: Appl. Phys.* **38**, 175 (2005).

²⁶S. A. Wilson, R. W. Whatmore, *J. Korean Phys. Soc.* **32**, 1204 (1998).

²⁷C. P. Bowen, R. E. Newnham, and C. A. Randall, *J. Mater. Res.* **13**, 205 (1998).

²⁸V. Tomer and C. A. Randall, *J. Appl. Phys.* **104**, 074106 (2008).

²⁹V. Tomer, C. A. Randall, G. Polizos, J. Kostelnick, and E. Manias, *J. Appl. Phys.* **103**, 034115 (2008).

³⁰S. A. Wilson, Ph.D. thesis, Cranfield University, 1999.

³¹T. B. Jones, *Electromechanics of Particles* (Cambridge University Press, Cambridge, UK, 1995).

³²A. Sihvola, *Electromagnetic Mixing Rules and Applications* (The Institution of Electrical Engineers, London, UK, 1999).

³³H. L. W. Chan and J. Unsworth, *IEEE Trans. Ultrason. Ferroelectr. Freq. Control* **36**, 434 (1989).

³⁴W. S. Rasband, IMAGEJ, U.S. National Institutes of Health, Bethesda, MD, <http://rsb.info.nih.gov/ij/index.html> (2007).

³⁵C. Ighathinathane, L. O. Pordesimo, E. P. Columbus, W. D. Batchelor, and S. R. Methuku, *Comput. Electron. Agric.* **63**, 168 (2008).

³⁶N. D. Spencer and J. H. Moore, *Encyclopedia of Chemical Physics and Physical Chemistry* (Institute of Physics Publishing, Bristol, UK, 2001).

³⁷S. Montserrat, F. Roman, and P. Colomer, *Polymer* **44**, 101 (2003).

³⁸R. A. Pethrick and D. Hayward, *Prog. Polym. Sci.* **27**, 1983 (2002).

³⁹R. A. Anderson, *Langmuir* **10**, 2917 (1994).

⁴⁰B. Techaumnat, B. Eua-arporn, and T. Takuma, *J. Phys. D: Appl. Phys.* **37**, 3337 (2004).

⁴¹H. P. Savakus, K. A. Klicker, and R. E. Newnham, *Mater. Res. Bull.* **16**, 677 (1981).